

Observation of resonance line narrowing for old muonium

M. G. Boshier,¹ S. Dhawan,¹ X. Fei,¹ V. W. Hughes,¹ M. Janousch,^{1,6} K. Jungmann,² W. Liu,¹ C. Pillai,⁴ R. Prigl,¹ G. zu Putlitz,² I. Reinhard,² W. Schwarz,¹ P. A. Souder,³ O. van Dyck,⁴ X. Wang,³ K. A. Woodle,⁵ and Q. Xu¹

¹Physics Department, Yale University, New Haven, Connecticut 06520-8121

²Physikalisches Institut, Universität Heidelberg, D-69120 Heidelberg, Germany

³Physics Department, Syracuse University, Syracuse, New York 13244

⁴Los Alamos National Laboratory, Los Alamos, New Mexico 87545

⁵Brookhaven National Laboratory, Upton, New York 11973

⁶Institute for Particle Physics, Eidgenössische Technische Hochschule Zürich–Honggerberg, CH-5232 Villigen PSI, Switzerland

(Received 14 November 1994)

Resonance line narrowing up to $\frac{1}{2}$ of the natural linewidth has been observed for microwave magnetic-resonance transitions between Zeeman levels of ground-state muonium at a strong magnetic field of 1.7 T. The observed lines are in good agreement with predicted line shapes and are useful for a precision determination of $\Delta\nu$ and μ_μ/μ_p .

PACS number(s): 36.10.Dr

An experiment is in progress at the Los Alamos Meson Physics Facility (LAMPF) to measure with higher precision the hyperfine structure interval $\Delta\nu$ and the Zeeman effect (or the ratio μ_μ/μ_p of the muon and proton magnetic moments) in muonium by the method of microwave magnetic-resonance spectroscopy [1]. The technique of resonance line narrowing [2] involving observation only of muonium atoms that have lived longer than their mean life of 2.2 μs is being used to help in achieving a higher-precision measurement than has been obtained thus far [3]. Statistically the loss in counting rate is more than compensated for by the narrower linewidth and the larger signal, and to minimize systematic errors the narrower linewidth is advantageous.

The energy-level diagram for $1^2S_{1/2}$ ground-state muonium in a magnetic field is shown in Fig. 1, which indicates the two transitions ν_{12} and ν_{34} observed at a high magnetic field of 1.7 T. The hfs interval $\Delta\nu$ is determined from the sum $\nu_{12} + \nu_{34}$ and the ratio μ_μ/μ_p from the difference $\nu_{34} - \nu_{12}$ [1]. The experimental setup is shown in Fig. 2. The μ^+ beam is produced from the LAMPF 800-MeV proton beam, which consists of 650- μs pulses at a repetition rate of 120 Hz with an average intensity of 0.9 mA. The fully polarized μ^+ beam of momentum 26.5 MeV/c from the LAMPF stopped muon channel passes through an $\vec{E} \times \vec{B}$ separator, which removes e^+ from the beam to a residual level of $e^+/\mu^+ \approx 0.03$. Downstream from the separator is an \vec{E} field chopper [4] to modulate the μ^+ beam, which gave an extinction ratio of about 0.025, defined as the rate of μ^+ admitted during the μ^+ beam-off time of 10 μs to the rate during the on-time of 4 μs . The chopped μ^+ beam passes into the magnetic field of the solenoid and then into the target vessel containing Kr at a pressure of 0.5 or 1 atm. The superconducting solenoid is a magnetic-resonance imaging magnet operating in persistent mode with a stability of 1 part in 10^8 to 1 part in 10^7 per hour. With the iron and current shimming kit provided, a field homogeneity of better than 1

ppm over a 20-cm-diam sphere was achieved. A normally conducting modulation coil with Cu windings allowed a magnetic-field change of 100 G and made it possible to observe resonance lines by scanning the magnetic field. Resonance lines were also taken by scanning the microwave frequency with a fixed magnetic field. The magnetic field was measured using NMR free-induction decay signals from protons in a water sample. A cylindrical microwave cavity in the pressure vessel can operate at 1.897 GHz (ν_{12}) in the TM110 mode or at 2.566 GHz (ν_{34}) in the TM210 mode. Decay positrons from the muons are observed downstream on axis in a positron telescope consisting of two 10-mm plastic scintillators that are operated in coincidence. The positron energy was cut off below 28 MeV by a 2.5-cm Al and a 7.2-cm polyethylene absorber.

Muonium is formed when muons are slowed down in the Kr gas, and since the muons are polarized, polarized muonium is formed. A microwave-induced transition be-

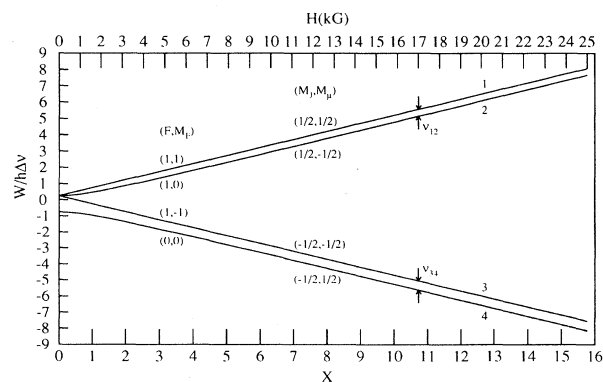


FIG. 1. Breit-Rabi energy-level diagram for the muonium $n=1$ ground state in magnetic field H . $\Delta\nu$ is the hfs interval and x is a dimensionless parameter proportional to H .

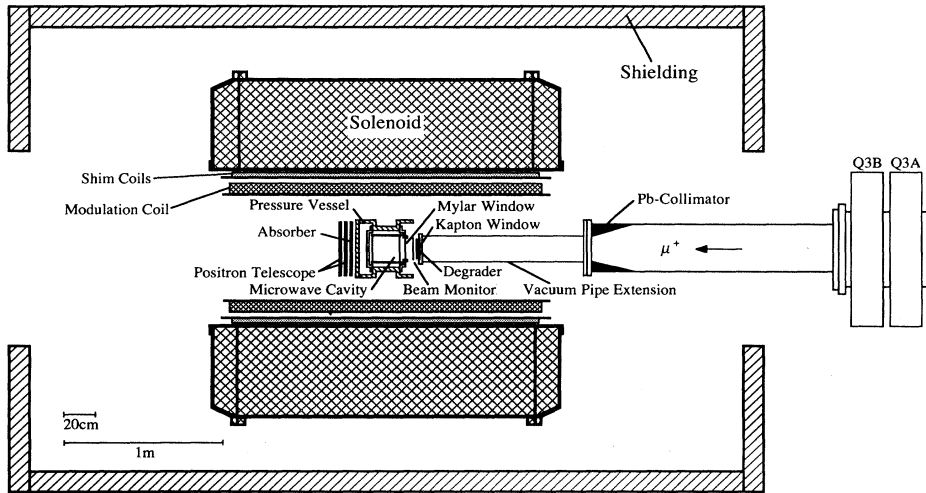


FIG. 2. Experimental setup for the LAMPF muonium experiment.

tween two states with different muon polarizations will change the number of positrons counted by the positron telescope because of the correlation of the direction of positron emission with the muon spin direction.

The resonance signals are a function of the magnetic field H and the microwave frequency ν [1],

$$S(\nu, H) = \frac{N_{\text{on}} - N_{\text{off}}}{N_{\text{off}}}, \quad (1)$$

in which N_{on} (N_{off}) is the number of e^+ counts with the microwaves on (off), normalized to the number of incoming muons. The conventional signal is defined as that obtained by counting positrons throughout the full beam-on time. The full width at half maximum of the resonance curve is given by

$$\delta\nu = \frac{1}{\pi} [\gamma^2 + 4|b|^2]^{1/2}, \quad (2)$$

$$\delta\nu = \frac{\gamma}{\pi} \quad \text{for } |b|^2 = 0, \quad (2a)$$

in which $\gamma = \mu$ decay rate $= 4.552 \times 10^5 \text{ s}^{-1}$ and $|b|^2$ is the square of the matrix element of the Hamiltonian for the magnetic interaction of muonium with the microwave magnetic field, and hence is proportional to the square of the amplitude of the microwave magnetic field H_1 . The timing diagram for observing the conventional resonance line is shown in Fig. 3(a).

Narrower resonance lines with higher signals but fewer events can be obtained by observing only muonium atoms that have lived longer than about 1 mean life of $\tau_\mu = 2.2 \mu\text{s}$. For magnetic-resonance transitions in the ground state of muonium, narrowed lines have been observed by the "old muonium" technique [5] and also by the similar separated oscillating fields technique [5,6]. As compared to the earlier study of "old muonium" resonance lines, the present observations involve transitions at strong magnetic field and, with the much reduced statistical uncertainties, narrowed lines can be seen with much longer time delays. For our experimental setup, the timing arrangement is shown in Fig. 3(b). Muons are admitted during $4 \mu\text{s}$, and subsequently during a $10\text{-}\mu\text{s}$ period

muons are deflected out of the beam by the chopper. Microwaves are on throughout this $14\text{-}\mu\text{s}$ period, but decay positrons are observed only in consecutive time intervals $t_2 - t_1$ of $2 \mu\text{s}$.

Observed conventional and "old muonium" lines for the transition ν_{12} obtained by scanning the field are shown in Figs. 4(a) and 4(b) and in Figs. 4(c)–4(f), respectively. For the conventional line at the transition frequency ν_{12} in Fig. 4(a) the μ^+ beam is not chopped, but

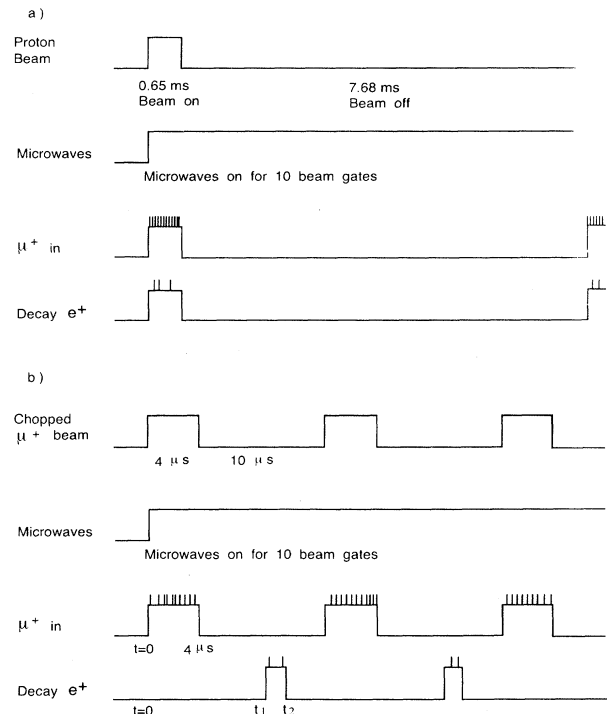


FIG. 3. (a) Timing diagram for observing a conventional resonance line. This time structure is that of the LAMPF proton beam and also of the muon beam. (b) Timing diagram for observing an "old muonium" resonance line. This time structure is imposed on the usual LAMPF muon beam by the chopper.

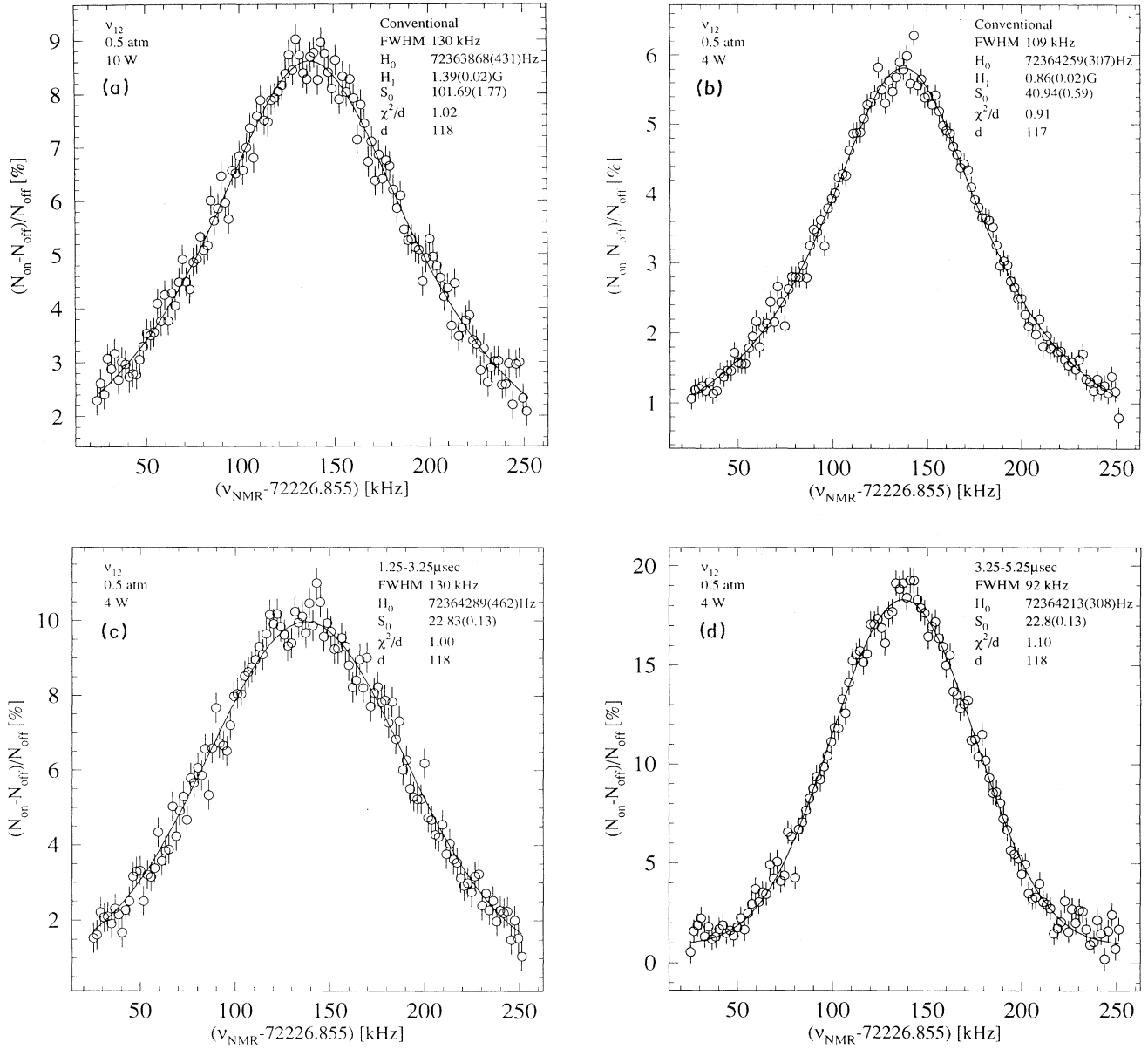


FIG. 4. Observed ν_{12} resonance lines obtained by magnetic-field scan with a 0.5-atm Kr target. (a) Conventional resonance line without the μ^+ beam chopped and with a microwave power of 10 W in the cavity. (b) Conventional resonance line with the μ^+ beam chopped and a microwave power of 4 W in the cavity. (c)—(f) Old muonium resonance lines with a microwave power of 4 W and different observation times measured from the beam-off time. The solid curves are fitted lines. The field H is the measured proton NMR frequency (4.26 kHz/G).

for that in Fig. 4(b) the μ^+ beam is chopped. Line narrowing of about a factor of 2.3 is observed from Fig. 4(a) (fractional width $\Delta H/H_0 = 1.9 \times 10^{-3}$) to Fig. 4(f) (fractional width $\Delta H/H_0 = 0.83 \times 10^{-3}$). The signal amplitude also increases for old muonium lines although the number of decay e^+ decreases as the observation time interval $t_2 - t_1$ is delayed. The conventional line of Fig. 4(a) is taken with a microwave power of 10 W in the cavity, whereas for Fig. 4(b) the power was 4 W. The ν_{34} resonance lines (not shown) exhibit the same general characteristics as the ν_{12} resonance lines.

The theoretical line shape for an old muonium line is

given in Eq. (3) [7],

$$S = S_0 \frac{L}{e^{-\gamma t_1} - e^{-\gamma t_2}}, \quad (3)$$

in which

$$L = \frac{2|b|^2}{\Gamma^2} \left[e^{-\gamma t_1} \left[1 - g(t_1) \frac{\gamma^2}{\Gamma^2 + \gamma^2} \right] - e^{-\gamma t_2} \left[1 - g(t_2) \frac{\gamma^2}{\Gamma^2 + \gamma^2} \right] \right], \quad (3a)$$

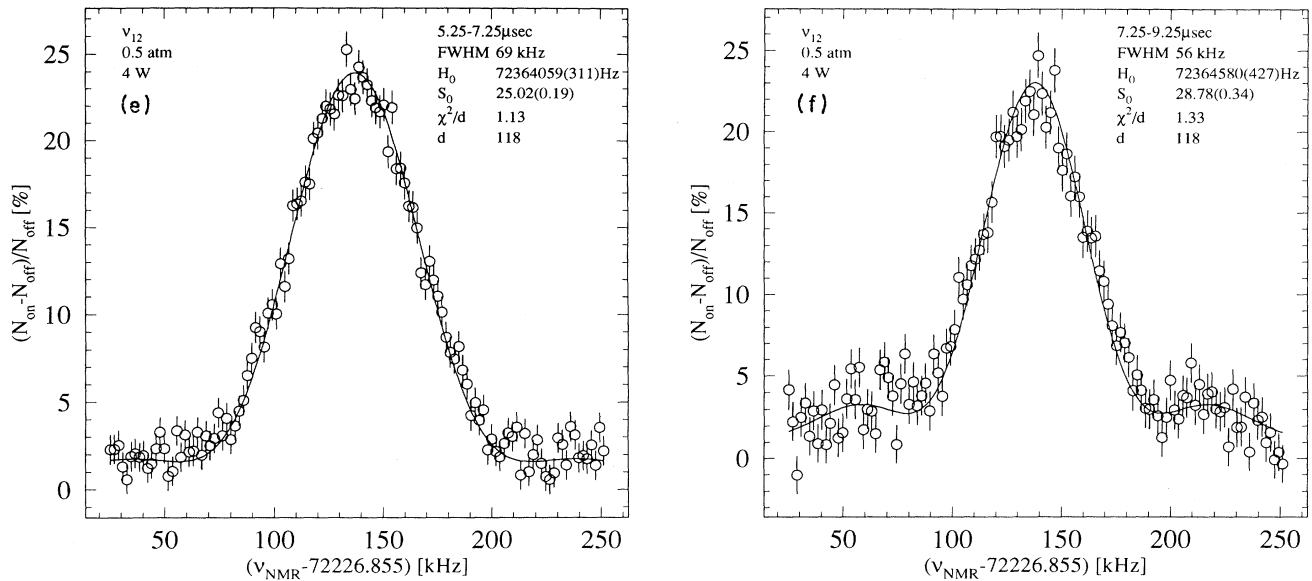


FIG. 4. (Continued).

where

$$g(t) = \cos \Gamma t - (\Gamma/\gamma) \sin \Gamma t, \quad (3b)$$

$$\Gamma^2 = \omega'^2 + 4|b|^2, \quad \omega' = \omega_{12} - \omega. \quad (3c)$$

S_0 is a constant, and t_1 (t_2) is the beginning (ending) observation time for decay positrons, measured from the time of muonium formation. It is clear from Fig. 3(b), which shows that μ^+ are admitted to the target for a 4- μs period, that a calculation of the theoretical line shape must involve integration over the times t_1 and t_2 .

Fitted theoretical line shapes are shown by the solid curves in Fig. 4. For Fig. 4(a), which is a conventional resonance line, as defined in Fig. 3(a), the theoretical line shape is given by Eq. (3) with $t_1=0$ and $t_2=\infty$. The fitting parameters are the line center H_0 , a scaling factor S_0 related to the maximum signal height and taking into account positron background, and the microwave field amplitude H_1 , which is proportional to $|b|$. The quantity $|b|$ together with the muon decay rate γ determine the resonance line width. Normalization of the incident muon beam intensity is based on a muon beam counter that integrates over the 0.65-ms period of the proton beam gate with a random error of about 0.1%. To an adequate approximation, Fig. 4(b) can also be considered a conventional resonance line for which the incident μ^+ beam is chopped, as indicated in Fig. 3(b), and e^+ are observed throughout the proton beam-on time.

Fits to the old muonium lines in Figs. 4(c)–4(f) are based on Eq. (3) together with integration over t_1 , t_2 and use the two fitting parameters H_0 and S_0 with the value of H_1 , taken from the fit to Fig. 4(b). Since the extinction ratio is not zero, the experimental line shape is composed of a relatively small conventional resonance line shape associated with the μ^+ beam not extinguished by the chopper, as well as the old muonium resonance line.

This conventional background line is chosen to be the fitted line for Fig. 4(b), with its amplitude corresponding to a 0.025 extinction ratio. The fits to the experimental lines in Figs. 4(c)–4(f) were done with several different values of the extinction ratio consistent with its measured value, as well as with several different values of the maximum time interval between the start of the beam-off chopper pulse $t=0$ and the time t_1 [see Fig. 3(b)], again with values consistent with measured values to account for the actual chopper pulse shapes.

For the fits, the field values H were the measured values at the center of the target corrected for diamagnetic shielding, and hence are absolute values accurate to 0.1 ppm. The field inhomogeneity of less than 1 ppm over the target was not considered. In addition, the muon stopping distribution and the microwave-field amplitude were taken to be constant. These approximations are reasonable for the study of the line shapes. For the later purpose of a precision determination of $\Delta\nu$ and μ_μ/μ_p , the actual variations of H , H_1 and the μ^+ stopping distribution must be considered.

The observed and fitted theoretical resonance lines in Figs. 4(a)–4(e) are in good agreement, as indicated by the values of χ^2/d shown on the figures, in which d is the number of degrees of freedom in the fit. Hence we confirm the expected general features of the old muonium lines, which include the line narrowing and the development of wings to the lines away from the central peak. For Fig. 4(f) the fit is unsatisfactory, as indicated by the large value of χ^2/d . The fit in the wings of the lines is particularly poor. For this old muonium line with the latest time window, the signal counts are small and the nonzero extinction ratio will have its largest effect, but we do not yet have a full quantitative explanation for this line shape. However, the expected line narrowing is clearly observed.

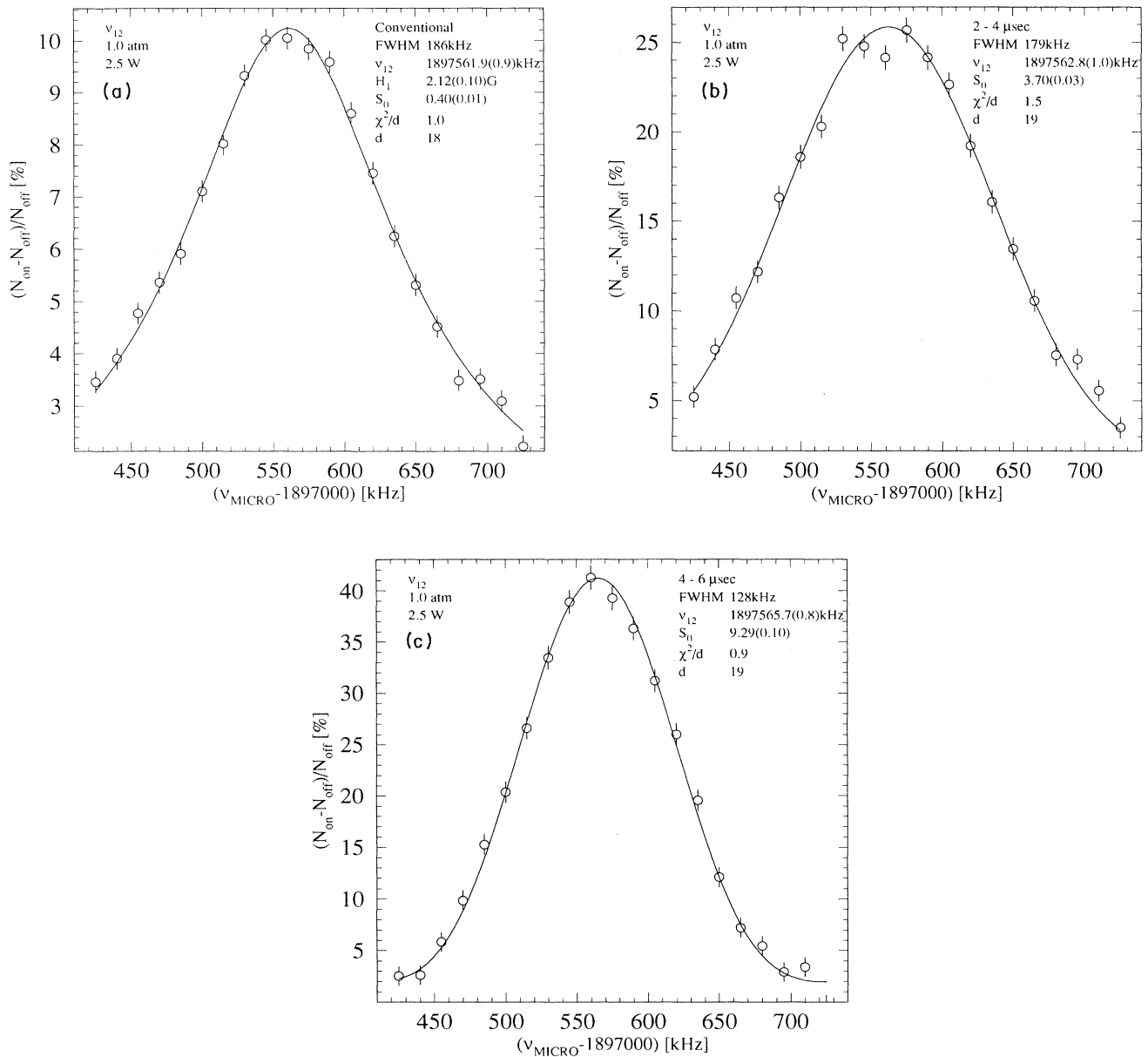


FIG. 5. Observed ν_{12} resonance lines obtained by a frequency sweep with a 1.0-atm Kr target. The chopped μ^+ beam was used for all figures. (a) Conventional line. (b)–(e) are old muonium lines. The solid curves are the fitted lines.

Resonance lines were also taken with variation of the microwave frequency for a fixed magnetic field. With a chopped muon beam, Fig. 5(a) shows a conventional line and Figs. 5(b)–5(e) show old muonium lines. The solid curves are fits to these lines based on Eq. (3) and done in the same manner as for Fig. 4. During the data-taking for these lines the magnetic field had an inhomogeneity of about 50 ppm over the cavity volume, and hence the fits were made with an approximate representation of the magnetic-field inhomogeneity and included the microwave field and muon stopping distributions. We believe that the variations of the fitted values for ν_{12} with the old muonium time window are associated with this

large field inhomogeneity. The fitted line shapes are in reasonable agreement with the observed lines. The old muonium line with the longest delay is narrower by a factor of 2.4 and has a larger signal by a factor of 4 compared with the conventional line of Fig. 5(a). The fractional linewidth is narrower with a frequency sweep as compared to a field sweep, as predicted by the Breit-Rabi equation.

For the resonance lines in Fig. 4 obtained by scanning the magnetic field, the old muonium resonance lines for the longest delays are narrower by a factor of 2.3 and have larger signals by up to a factor of 2.5, as compared to a conventional resonance curve obtained with an un-

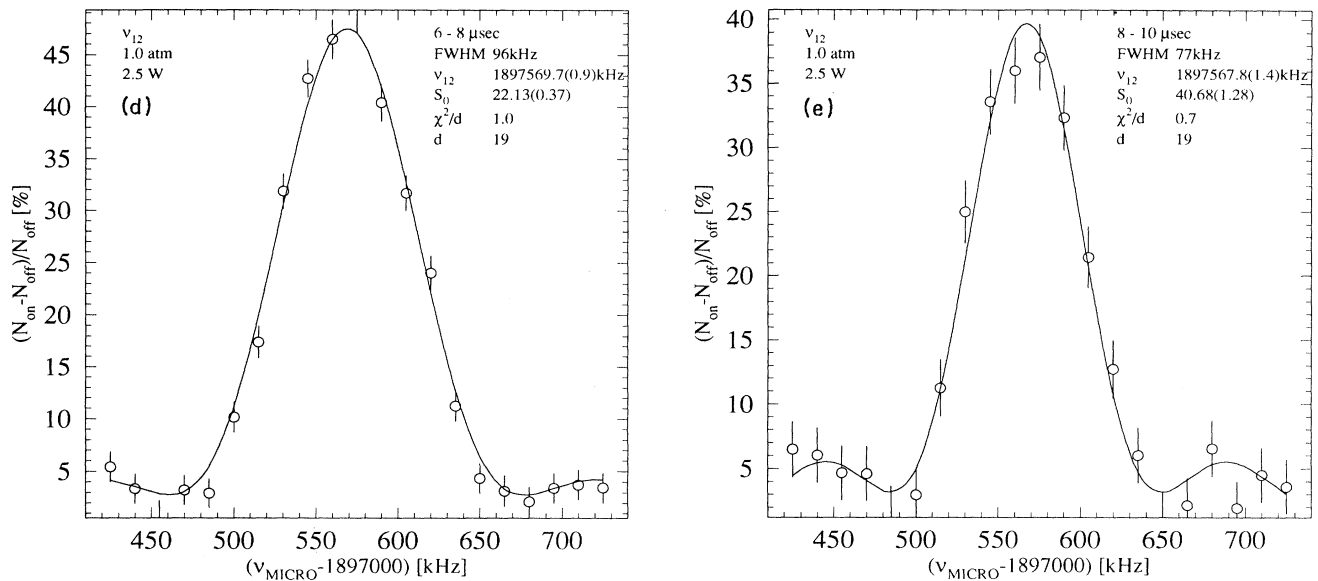


FIG. 5. (Continued).

chopped muon beam. However, the counting rate is reduced by up to a factor of about 200 for the latest time bin. Taking into account all four time bins from the old muonium mode, as well as the conventional line obtained simultaneously, about 50% more running time is needed with the conventional unchopped mode as compared to the old muonium mode to achieve the same statistical accuracy with the same incoming μ^+ beam. From the viewpoint of systematic errors, which are often proportional to the linewidth, it is advantageous to have narrower lines.

We are happy to acknowledge the excellent operation of the LAMPF proton beam and muon beam under the

direction of E. Hoffman and R. Werbeck. We are also indebted to E. Hoffman, D. Fitzgerald, A. Browman, and P. Foy for providing a muon beam chopper, and to L. Willmann and U. Haerberlen of Heidelberg for contributing to the NMR magnetometer, and to A. Disco of Yale for mechanical design. Finally we thank C. Hoffman for his overall help, encouragement, and good judgment. Research was supported in part by the U.S. Department of Energy, Bundesministe für Forschung und Technologie (Germany), and a NATO Research Grant. R.P. and W.S. would like to thank the Alexander von Humboldt Foundation, the Feodor Lynen Program, and the Max Kade Foundation for financial support.

- [1] V. W. Hughes and G. zu Putlitz, *Quantum Electrodynamics*, edited by T. Kinoshita (World Scientific, Singapore, 1990), p. 822.
- [2] V. W. Hughes, *Quantum Electronics*, edited by C. H. Townes (Columbia University Press, New York, 1960), p. 582; G. zu Putlitz, *Comments on At. Mol. Phys.* **1**, 74 (1969).

- [3] F. G. Mariam *et al.*, *Phys. Rev. Lett.* **49**, 993 (1982).
- [4] D. Ciskowski *et al.*, *Nucl. Instrum. Meth. A* **333**, 260 (1993).
- [5] D. E. Casperson *et al.*, *Phys. Lett.* **59B**, 397 (1975).
- [6] D. Favart, *et al.*, *Phys. Rev. A* **8**, 1195 (1973).
- [7] W. E. Cleland, *et al.*, *Phys. Rev. A* **5**, 2338 (1972).